Performance Prediction Correlations Resulting from a Fundamental Fin Coiled Heat Exchanger

L. Makaum, P.v.Z. Venter and M. van Eldik

***Abstract*—**This paper investigated an industrial size air-to-water fin coiled heat exchanger. Uncertainties in heat transfer predictions result in over or under sizing. However, a simulation model was developed, incorporated the Nusselt number correlation of Zukauskus, proving to be accurate. Experiments were performed at various water and air flow rate ranges, for a variety of ambient air temperatures.

The finned heat exchanger consists out of an aligned tube configuration. The simulation requires the water and air side's input parameters to predict the output values. The simulated air side convection heat transfer coefficient was compared to test data. The largest percentage error was found to be within 12.00%.

Three guideline correlations were furthermore developed from the test results. These correlations are used to calculate the output temperatures of the water and air, as well as the average air side convection heat transfer coefficient, with a maximum convection heat transfer error of 13.36%.

***Keywords*—**Nusselt number correlation; e-NTU; heat exchanger; heat transfer; simulation; fundamental principles.

I. Introduction

A temperature difference between two mediums (liquid, gas or solid) will result in a transfer of energy in the form of heat. The flow of heat will always take place from the medium with the higher temperature to the medium with the lower temperature according to the second law of thermodynamics, [1].

There are three mechanisms for the transfer of thermal energy: conduction through a solid or a fluid in a stationary condition, convection from a stationary surface to a moving fluid and a net radiation exchange between two surfaces at different temperatures. A heat exchanger is used to transfer thermal energy between various mediums, where the fluids are typically separated by a thin conducting wall.

There are different types of heat exchangers for various applications classified by the flow arrangement and construction [2]. For the flow arrangement there exist parallel flow, counter flow and cross flow. Each of these flow arrangements leads to different heat exchanger characteristics and therefore performance. For this study cross flow heat exchangers will be investigated. The process of heat transfer between two fluids can be seen in various engineering applications such as power production, waste heat recovery, chemical processing and air-conditioning, to name a few [2].

The addition of fins on the exterior of the coil increases the area for convective heat transfer to the air moving through the heat exchanger. In these extended surfaces the direction of the heat transfer from the boundaries (convection) is perpendicular to the heat transfer trough the solid (conduction), [2]. When fins are applied to the coils the convective heat transfer coefficient will increase which will in turn increase the overall heat transfer rate.

Although a great quantity of heat exchanger exist on the market having different shapes and sizes, there units' performances are difficult to predict. This is due to the complexities associated with the heat exchangers including the geometry, the flow of the air through the different pipe arrangements, the water flow path, and the heat transfer rate at different points. Considering these complexities, no analytical solution exist to determine the performance of such a heat exchanger.

One of the first studies performed were on the heat transfer of laminar flow within a duct of various shapes in a closed channel in 1883, [3]. This research was then independently continued by Wilhelm Nusselt in 1910. After this several literature were published for different shapes and sizes. A further refinement on this literature focused on the analytical solutions of the Nusselt number for different shapes of ducts where only laminar flow exist. These solutions were only applicable when there is a constant heat flux through the walls or the temperature of the wall is kept at a constant value. These analytical approaches used mathematical techniques such as Galerkin integral methods, [4], and conformal mapping, [5]. Due to the complexity of heat exchangers and the different operating conditions, generic analytical solution were not obtainable. Thus simplified models of the heat exchanger for different operating conditions were introduced. This was still an analytical approach with the idea in mind to take a fixed operating condition and compensating for it within the mathematical model. The air-side performance of a single phase heat exchanger with louvered fins were approached analytically with further studies, [6].

This model was used to predict the performance of single phase heat exchangers with louvered fins focusing on the heat transfer coefficients. These coefficients had errors of approximately 25%. Another analytical approach for a

P.v.Z. Venter is with the School of Mechanical and Nuclear Engineering, North-West University. Potchefstroom, South-Africa .

L. Makaum was with School of Mechanical and Nuclear Engineering, North-West University. Potchefstroom, South-Africa (12330825@nwu.ac.za).

M. van Eldik, School of Mechanical and Nuclear Engineering, North-West University. Potchefstroom, South-Africa.

simplified model was introduced. This model included the calculation of the heat transfer at the air-side of a heat exchanger where the working fluid undergoes condensation as proposed by [7].

The condensation of the working fluid was further investigated with regards to compact heat exchangers by. Most of these analytical approaches do not give adequate results for the design process of thermal systems [8].

II. EXPERIMENTAL APPARATUS

The layout of the test bench can be seen in Fig. 1. The test bench allows for ambient air to circulate through a duct. Fans are installed in this arrangement to create a suction effect which results in the movement of air through the heat exchanger. Different measuring devices are used to obtain the properties of the air and water at different stages in the test bench. For this purpose a number of temperature and pressure probes have been installed.

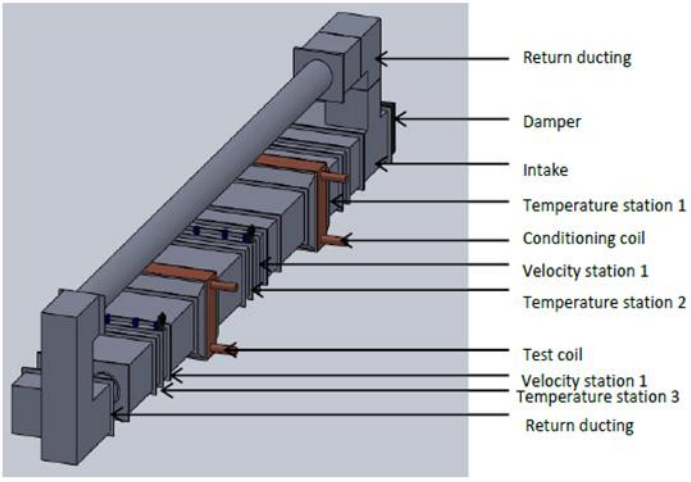

Fig 1 Layout of test bench [9].

There are two coils placed in the test bench: the test coil and the conditioning coil.

The purpose of the conditioning coil is to change the air temperature to different values so that the test coil can be tested at different air temperatures. The test coil is the main focus of the test bench and thus the properties of the fluids will be evaluated for this coil.

The water used in this test bench is heated by means of a heat pump. This water is contained in a reservoir tank which can hold approximately 5 kiloliters of water. A mixing bench, containing two pumps in series, is then used to supply the test bench with warm water.

There are four fans situated at the exit of the test coils. A PLC system is used to control the fans and allows for different configurations. One of the fans is also controlled by a VSD which means that it can be set to different speeds. The other three fans only have an on/off command.

The coils are placed within the duct allowing cold air to move through the coil while warm water moves through the pipes. This allows for heat exchange between the air and the water. The dampers are used to regulate the air flow out of the system and thus also regulates the air moving in the return duct. These dampers are controlled by the PLC system and can be set to different percentages. The return ducting is used to circulate the ambient air within the test bench system. The temperature of the water and air at the inlet and outlet of the heat exchanger is measured with PT100 temperature probes and psychrometers respectively. A positive displacement flow meter is used to measure the volumetric flow rate of the water while pressure sensing probes are used to determine the dynamic pressure of the air from which the velocity can be calculated.

III. THEORY

In this section the fundamental equations and definitions necessary for the simulation model are given. Only the most important components are discussed [10],[11].

A. Conservation Laws

For a finite control volume the integral form of the conservation of mass is defined as:

$$\frac{\partial}{\partial t}\left(\iiint \rho d\mathcal{V}\right) + \oiint \rho \bar{V} \cdot \overline{dA} = 0 \quad (1)$$

Where ρ is the density, $\mathcal{V}$ is the volume, V is the velocity relative to the control volume and A is the area.

The integral form of the linear momentum conservation equation is given as:

$$\oiint \tau \overline{dA} + \iiint \bar{B}\rho d\mathcal{V} = \frac{\partial}{\partial t}\left(\iiint \bar{V}\rho d\mathcal{V}\right) + \oiint \bar{V}\left(\rho \bar{V} \cdot \overline{dA}\right) \quad (2)$$

Where τ is the shearing stress and B is the body forces acting upon the control surface.

And for the conservation of energy:

$$\dot{Q} + \dot{W} = \frac{\partial}{\partial t}\left(\iiint \left(u + \frac{1}{2}V^2 + gz\right)\rho\, d\mathcal{V}\right) + \oiint \left(h + \frac{1}{2}V^2 + gz\right)\rho \bar{V} \cdot \overline{dA} \quad (3)$$

Where $\dot{Q}$ is the rate of heat transfer to the control volume and $\dot{W}$ is the work done on the control volume.

B. Heat Transfer

The heat transfer between two fluid increments are obtained from the effectiveness-NTU ($\epsilon - NTU$) method.

The heat capacity rates for the hot and cold fluid is given as:

$$C = \dot{m} c_p \quad (4)$$

Where C is the heat capacity rate, $\dot{m}$ is the mass flow rate and c_p is the constant pressure specific heat of either the cold or cold fluid.

We then define the smaller heat capacity as C_{min} and the larger quantity as C_{max}.

The heat capacity ratio is defined as:

$$C_r = \frac{C_{min}}{C_{max}} \quad (5)$$

A dimensionless parameter called the *number of transfer units* (NTU) is used in a variety of heat exchanger problems. This parameter is defined as follows:

$$NTU = \frac{UA}{C_{min}} \quad (6)$$

Where UA is the product of the overall heat transfer coefficient and the area of either the hot or cold side.

For a cross flow heat exchanger (single pass) the effectiveness can be calculated using the following equation:

$$\varepsilon = 1 - \exp\left(\left(\frac{1}{C_r}\right)(NTU)^{0.22}\{\exp\left[-C_r(NTU)^{0.78}\right] - 1\}\right) \quad (7)$$

The maximum possible heat transfer rate is defined as follows:

$$\dot{q}_{max} = C_{min}(T_{h,i} - T_{c,i}) \quad (8)$$

To calculate the heat transfer the following equation will then be applied:

$$\dot{q} = \varepsilon \dot{q}_{max} \quad (9)$$

Where $\dot{q}$ is the heat transfer between the fluids for the segment.

C. Nusselt Number and Pressure Drop

For turbulent flow ($Re \geq 10^4$) within a cylindrical tube the **Dittus-Boelter** correlation can be used:

$$Nu = 0.023 Re^{0.8} Pr^n \quad (10)$$

Where n is equal to 0.4 when the fluid inside the tube is heated and n equals 0.3 when the fluid is cooled.

The pressure drop within the pipe can be described as:

$$\Delta p_{oL} = f \frac{L}{D_H} \frac{1}{2} \rho V^2 \quad (11)$$

f is known as the *Darcy-Weisbach* friction factor

This factor for turbulent flow ($5 \times 10^3 \leq Re \leq 10^8$ *and with* $10^{-6} \leq \frac{\varepsilon}{D_H} \leq 10^{-2}$) is defined as:

$$f = 0.25 \left(\log\left(0.27 \frac{\varepsilon}{D_H} + \frac{5.74}{Re^{0.9}}\right)\right)^{-2} \quad (12)$$

Where ε is the roughness of the surface.

For a tube bank the average heat transfer coefficient can be calculated using the Nusselt correlation proposed by Zukauskus [12]:

$$Nu = C_1 C_2 Re_{D,max}^m \mathrm{Pr}^{0.36} \left(\frac{Pr}{\mathrm{Pr}_s}\right)^{\frac{1}{4}} \quad (13)$$

Where Pr and Pr_s are the Prandtl numbers evaluated at the mean and surface temperatures and C_1 and C_2 are constants evaluated from the appropriate tables compensating for the shape and number of rows, respectively. $Re_{D,max}$ refers to the maximum Reynolds number in the tube banks which depends on the geometry and arrangement of the heat exchanger.

The pressure drop over a tube bank can be calculated as follows [11]:

$$\Delta p = N_L X \left(\frac{\rho V_{max}^2}{2}\right) f_a \quad (14)$$

Where N_L is the number of tubes in one column. The friction factor, f_a, and correction factor, X, are evaluated from figures for either aligned or staggered arrangements. It is important to note that the calculation of the pressure drop in this study does not require specific graphs for specific heat exchangers (as necessary in [13]), but only the knowledge of the type of arrangement.

IV. Simulation using fundamental laws

For the simulation program only the inlet conditions are allowed to be entered. The simulation program calculates the expected outlet conditions and the simulated convection heat transfer coefficient (*h*).

TABLE I :
DIMENSIONAL CHARACTERISTICS OF COIL.

Property	Dimension
Frontal width of coil	1.2 m
Height of coil	60.96 cm
Length of coil	24.6 cm
Thickness of pipe	0.3 mm
Outer tube diameter	1.26 cm
Fin pitch	6.35 mm
Fin thickness	0.18 mm
Fin efficiency	85 %
Vertical distance between tubes	38.1 mm
Horizontal distance between tubes	66 mm

The test coil used for this study is an aligned finned heat exchanger consisting out of sixteen rows and four columns of tubes. This means that the hot water moves from one side to another four times. The total mass flow is divided into sixteen separate pipes and only joins up again at the exit of the heat exchanger. The hot water enters at the one side while the cold air enters from the other side of the heat exchanger. Table 1 shows the physical dimensions of the heat exchanger.

To model the heat exchanger only a single row simulation is necessary. The reason for this is that when the water splits up at the entrance of the heat exchanger it does not touch each other until the exit of the heat exchanger. This means that each row works separately. Fig. 2 shows the pipe line that was simulated in this study. The fins of the heat exchanger are omitted in the drawing, but plays a vital role in the simulation.

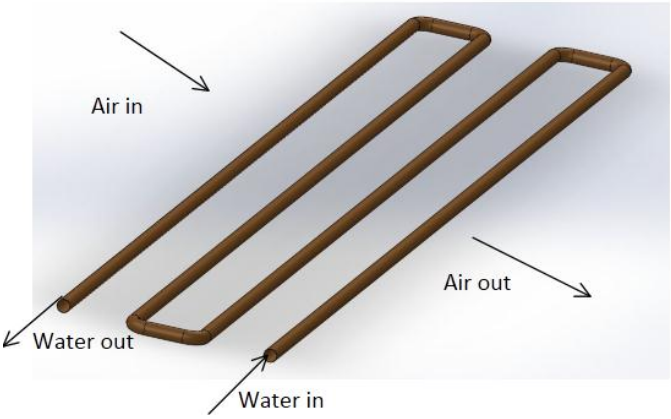

Fig 2 Simulated row of heat exchanger

The simulation is obtained by dividing this pipeline in multiple increments and applying the necessary conservation laws, component characteristics, fluid properties and boundary values to each.

V. Experimental conditions and data reduction

A. Experimental Conditions

The heat exchanger was tested at two different ambient temperatures with three different air velocities and three different water mass flow rates. Thus, the heat exchanger was tested at eighteen different conditions.

TABLE II
TEST DATA FOR ONE TEMPERATURE RANGE

Ambient temperature: 21 - 23 °C, Water temperature: 39 - 41 °C						
Flow rate: water	Air velocity [m/s]	Air inlet temp. [°C]	Air outlet temp. [°C]	Water inlet temp. [°C]	Water outlet temp. [°C]	Error [%] $\left\lvert\frac{Q_{water}-Q_{air}}{Q_{water}}\right\rvert$
25 l/min	2	21.52	29.57	38.9	31.11	5.92
	4	21.64	26.5	37.95	29.09	5.64
	6	21.84	25.9	38.11	28.2	4.97
50 l/min	2	21.74	32.06	40.41	35.02	5.63
	4	22.14	29.88	41.91	34.72	5.43
	6	22.69	28.1	41.15	32.8	5.87
75 l/min	2	21.58	32.3	40.52	36.5	3.04
	4	22.08	29.9	40.3	34.9	3.49
	6	22.76	29.3	41.5	34.7	4.74

Table 2 shows the results obtained for one of the tested air temperature ranges. The error refers to the difference between the heat absorbed by the air and the heat rejected by the water with reference to the waterside.

B. Data Reduction

The inlet and outlet values of the two fluids are known. To obtain the tested convection heat transfer coefficient on the air side the average water temperature of the segment must be determined (T_{ave}).

$$T_{ave} = \frac{T_{water,in} + T_{water,out}}{2} \quad (15)$$

Using the average temperature the Prandtl number (Pr), dynamic viscosity (μ), thermal conductivity (k) and density (ρ) are calculated. The Reynolds number (Re) is then calculated.

$$Re = \left|\frac{\dot{m} D_H}{\mu A_{ff}}\right| \quad (16)$$

Where D_H is the hydraulic diameter and A_{ff} is the free flow area. Using the equation (10) the Nusselt number (Nu) is calculated from which the average convection heat transfer coefficient (h) will be calculated.

$$Nu = \frac{h_c L_{char}}{k} \quad (17)$$

L_{char} is the characteristic length. The entire pipeline will be treated as one segment. The convection heat transfer coefficient for the simulation will be obtained by calculating the average convection coefficients for all the increments.

VI. RESULTS AND DISCUSSION

In this section the comparison between the experimental and simulated data are shown. In the following figures the tested and simulated exit temperatures of the water and air together with the percentage error of the simulated results are plotted. These figures only show the results for one temperature range. All of the percentage errors are below 1.5 %.

For the air exit temperatures it can be seen that the percentage error starts to increase as the air velocity increases. This may be due to the fact that the air starts to become more turbulent as the air velocity increases and then the temperature reading device becomes inaccurate.

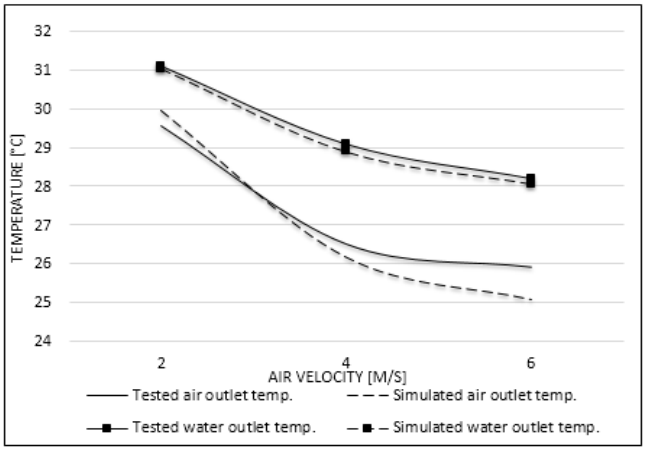

Fig 3 Simulated vs. tested: outlet temperatures 21 – 23 °C – 25 l/min

As the velocity of the air increases, resulting in a higher mass flow rate, the exit temperatures of the water and air decreases. Even though the air moves faster over the fins, the increase in molecules and turbulence allow for a higher total heat transfer rate. Note that this will not necessarily always be the case.

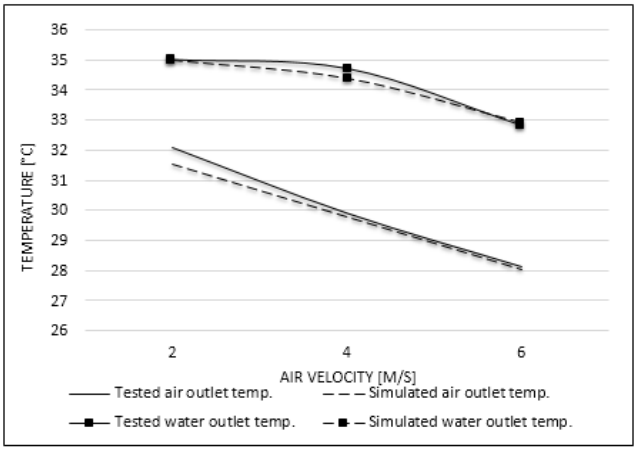

Fig 4 Simulated vs. tested: outlet temperatures 21 – 23 °C – 50 l/min

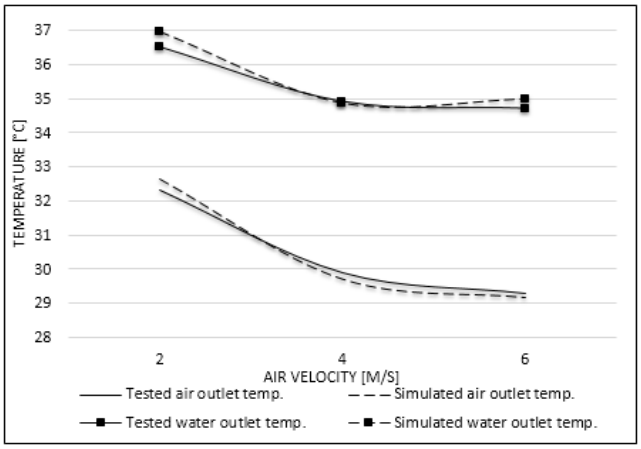

Fig 5 Simulated vs. tested: outlet temperatures 21 – 23 °C – 75 l/*min*

The air side convection heat transfer coefficient as a function of air velocity is given in figures 6 and 7. It should be noted that the convection coefficient for the simulation is calculated by taking the average of the convection coefficients of all the segments into which the pipe line was divided. The convection coefficient for the test results on the other hand was

calculated by assuming that the entire row of piping is stretched in to one long pipe and then using the e-NTU method. For this reason the results may have a larger error than seen at the outlet temperatures. In Fig. 6 the air side convection heat transfer coefficient as a function of air velocity at 25 l/min water flow rate is shown. It can clearly be seen that as the air velocity increases, the convection coefficient will also increase. This means that the faster the air is moving though the heat exchanger and over the pipes, the more heat will be exchanged. The simulated results shows a linear incline whereas the tested results shows a slight skew. This may be due to small inaccuracies of the measuring devices. The maximum error between the tested and simulated results is below 12.00 %.

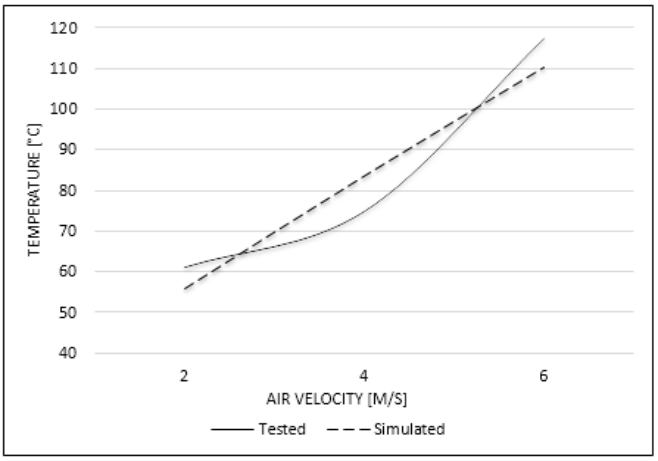

Fig 6 Convection heat transfer coefficient (air side), 21 – 23 °C, 25 l/min

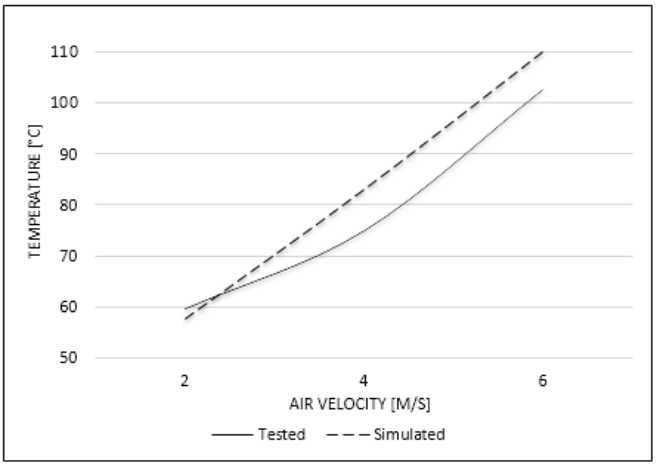

Fig 7 Convection heat transfer coefficient (air side), 21 – 23 °C, 50 l/min

When the simulated results were compared with the experimental obtained values, the percentage error increased as the air velocity increased. This may be due to the turbulence increases at higher air velocities or measuring uncertainties.

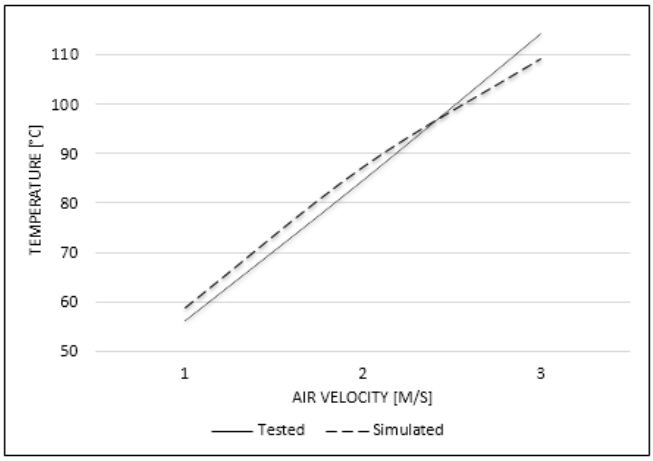

Fig 8 Convection heat transfer coefficient (air side), 21 – 23 °C, 75 l/min

VII. Correlations For Outlet Temperatures And Convection Coefficients

Correlations that can be used to predict the outlet temperature of the water and the air as well as another correlation to obtain the average air side convection heat transfer coefficient were developed from the experimental results. These equations can be used for a heat exchanger sizing guide without performing a full scale simulation. Such correlations will not attain the same accuracy as a simulation model but might prove a valuable decision making tool for manufacturing guidelines. Equations were derived for the outlet air and water temperatures, including the air's side convection heat transfer coefficient. Note that these correlations may only be applied to the specific coiled type heat exchanger used for the simulation model.

The equations are:

$$T_{out,water} = \alpha + \beta Y + \gamma X + T_{in,water} \quad (18)$$

$$T_{out,air} = \alpha + \beta Y + \gamma X + T_{in,air} \quad (19)$$

$$h_{air,side} = \alpha + \beta Y + \gamma X \quad (20)$$

Where Y is the volume flow rate of the water $\left[\frac{l}{min}\right]$, X is the velocity of the air $\left[\frac{m}{s}\right]$ and T_{in} is the inlet temperature of the water/air $[°C \text{ or } K]$. And:

Table III
Coefficients for correlation equations

Equation	α	β	γ
18	−8.583	0.076	−0.685
19	7.93345	0.06333	−1.058333
20	27.745	0.0574Y	13.3

Fig. 9 and 10 shows the comparison between the tested and correlated values for the outlet temperatures and convection heat transfer coefficient for one volume flow rate and ambient temperature. The maximum error found for the outlet temperatures were 3.13% while the maximum error for the heat transfer coefficient were 13.36%.

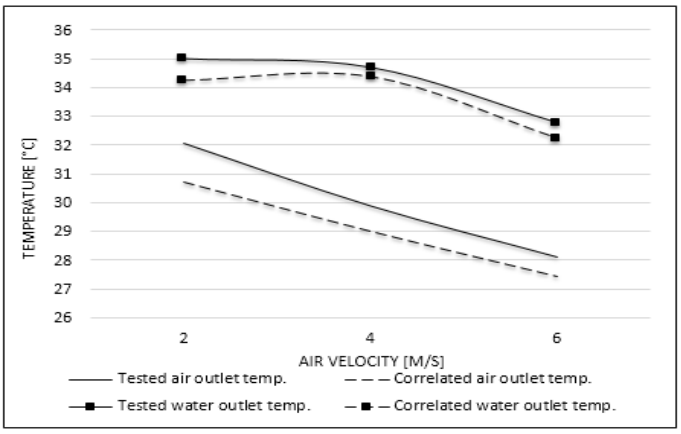

Fig 9 Correlated vs. tested: outlet temperatures 21 – 23 °C – 50 l/min

These correlations are only proven valid in the temperature ranges as seen in this study and can be used as a quick alternative to roughly estimate the output parameters of this specific heat exchanger.

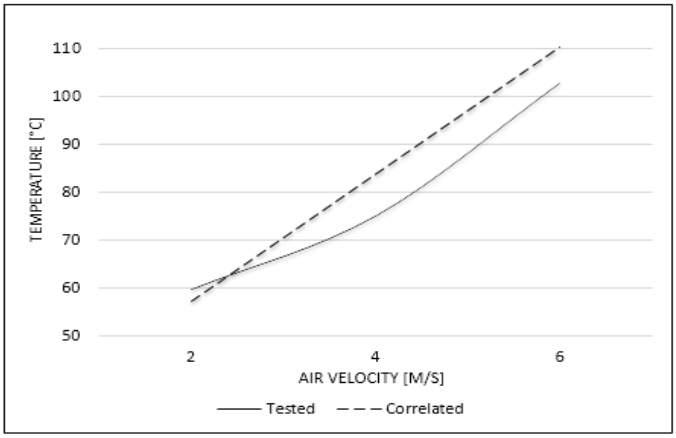

Fig 10 Convection heat transfer coefficient (air side), 21 – 23 °C, 50 l/min

VIII. Conclusions

A simulation model for a finned coiled heat exchanger was developed. The simulation proved to predict the convection heat transfer coefficients accurately within 12.00%. This means that the simulation program can be used to model and predict the outlet temperatures of both the water and air side of the heat exchanger. From the experimental data correlations were developed that may only be used within the operational test range of the data. These mixed linear equations can be utilised to determine the outlet temperatures for the air and water side, including the total convection heat transfer coefficients within a 13.36% accuracy interval.

Such equations are useful in the manufacturing context, allowing an accurate working prediction for the heat exchanger.

References

[1] R.D. James, J.M. (1979). The second law of thermodynamics and stability: Volume 70. Springer.

[2] Frank P. Incropera, D. P. (2013). Principles of Heat and Mass Transfer: Seventh edition. John Wiley & Sons.

[3] Shah, R. a. (1978). Laminar Forced Convection in Ducts. New York: Advances in Heat Transfer.

[4] Mashena M., H.-S. A.-S. (1983). Heat transfer coefficient in ducts with constant wall temperature vol. 105. ASME Journal of Heat Transfer.

[5] Sastry, R. (1964). Solution of the heat transfer of laminer forced-convection in non-circular pipes. Applied Science and Research, Vol. A3.

[6] Sahnoun A., a. W. (1992). Prediction of heat transfer and friction for the louver fin geometry. ASME Journal of Heat Transfer, Vol. 114.

[7] Ramadhyani, S. (1998). Calculation of air-side heat transfer in compact heat ex-changers under condensing conditions. South Hampton, UK: Computational Mechanics Publications.

[8] Srinivasan, R., & Shah, V. (1997). Condensation in compact heat exchangers. Journal of Enhanced Heat Transfer, Vol. 4.

[9] Bann, M. (2015). Analysis regarding the accuracy of the instrumentation installed on a Finned Coil Heat Exchanger Test Bench. Potchefstroom.

[10] Rousseau, P. G. (2013). Thermal-fluid systems modelling I (MGII885). Potchefstroom: North-West University.

[11] Frank P. Incropera, D. P. (2013). Principles of Heat and Mass Transfer: Seventh edition. John Wiley & Sons.

[12] Zukauskas, A., "Heat Transfer from Tubes in Cross Flow," in J.P. Hartnett and T.F. Irvine, Jr., Eds., Advances in Heat Transfer, Vol. 8, Academic Press, New York, 1972.

[13] Kays, W.M., and A.L. London, Compact Heat Exchangers, 3rd ed., McGraw-Hill, New York, 1984